ELSEVIER

The friction coefficient of a fully developed laminar reciprocating flow in a circular pipe

T. S. Zhao and P. Cheng
Department of Mechanical Engineering, The Hong Kong University of Science and Technology, Clear Water Bay, Kowloon, Hong Kong

Pressure drops in a fully developed laminar incompressible reciprocating pipe flow have been investigated analytically and experimentally. An exact analytical solution for the instantaneous and cycle-averaged friction coefficients of a fully developed laminar reciprocating flow has been obtained. It was found that, although the dimensionless axial velocity profiles of a fully developed flow depend only on the kinetic Reynolds number, the friction coefficients depend not only on the kinetic Reynolds number but also the dimensionless oscillation amplitude of fluid. Experiments have been carried out to measure the pressure drops of a laminar reciprocating flow at downstream of a long pipe at various frequencies and fluid displacements. Comparisons are made for the time-resolved and the cycle-averaged friction coefficients between the analytical solution and experimental data. It is shown that the analytical solution is in good agreement with measurements.

Keywords: reciprocating flow; friction coefficient; kinetic Reynolds number; dimensionless oscillation amplitude of fluid

Introduction

The problem of oscillatory flow in a pipe under the influence of periodic pressure fluctuations has been studied by many researchers both analytically and experimentally. Measurement by Richardson and Tyler (1929) first indicated that the maximum axial velocity in a fast oscillatory flow occurs near the wall, which is the "annular effect." Sexl (1930) and Womersley (1955) later verified the "annular effect" by performing analyses for both sinusoidal and nonsinusoidal motions of a fully developed incompressible laminar oscillatory flow in a pipe. Uchida (1950) obtained velocity profiles of a fully developed incompressible laminar pulsating flow (with nonzero mean velocity) in a straight pipe for an externally imposed nonsinusoidal pressure gradient. Most recently, Akhaven et al. (1991) experimentally verified Uchida's analytical solution by measuring velocity profiles of a reciprocating flow of water in a pipe.

Relatively few papers have reported on the study of frictional losses in a reciprocating pipe flow. Roach and Bell (1988) obtained some data of pressure drops and heat transfer in a tube and a packed tube under rapidly reversing flow conditions. They reported higher friction factors but could not find frequency dependence in either pressure drop or heat transfer data. Wu et al. (1990) performed experiments on the friction factor in a gap heat exchanger and presented their data versus the Reynolds number at given values of the oscillation frequency. Taylor and Aghili (1984) gathered some data of pressure drops in an oscillating flow of water in a pipe of a finite length at relatively low frequencies. Their data indicate an increase of the friction coefficient over an unidirectional steady flow. However, they did not have sufficient data to investigate the effects of frequency on the friction coefficient.

The purpose of the present work is twofold. First, to obtain an analytical expression for predicting the friction coefficient of a fully developed reciprocating pipe flow (with zero mean velocity) based on Uchida's (1950) solution for a pulsating flow (with nonzero mean velocity). Second, to compare this expression with experimental data obtained by measuring temporal variations of axial cross-sectional mean velocity and pressure drops downstream of the pipe using a hot-wire anemometer and a differential pressure transducer, respectively. It is expected that the results reported herein will be useful for predicting friction losses in the design of heat exchangers in a Stirling engine or a pulse-tube cryocooler.

Analytical solution

Consider a hydrodynamically fully developed reciprocating flow in a pipe with diameter D. The governing conservation equations of mass and momentum for an incompressible fully developed flow are

$$\frac{\partial u}{\partial x} = 0 \tag{1}$$

$$\frac{\partial u}{\partial t} = -\frac{1}{\rho}\frac{\partial p}{\partial x} + \nu\left(\frac{\partial^2 u}{\partial r^2} + \frac{1}{r}\frac{\partial u}{\partial r}\right) \tag{2}$$

where x and r are the axial and radial coordinates, u is the axial velocity, p is the pressure, and ρ and ν are the density and the kinematic viscosity of fluid, respectively.

Address reprint requests to Prof. P. Cheng, Department of Mechanical Engineering, The Hong Kong University of Science and Technology, Clear Water Bay, Kowloon, Hongkong.

Received 25 July 1995; accepted 27 December 1995

Int. J. Heat and Fluid Flow 17: 167–172, 1996

655 Avenue of the Americas, New York, NY 10010

0142-727X/96/$15.00
SSDI 0142-727X(96)00001-5

We now assume that the reciprocating flow is driven by a sinusoidally varying pressure gradient given by

$$\frac{1}{\rho}\frac{\partial p}{\partial x} = k \cos \omega t \tag{3}$$

where k and ω are the amplitude and the circular frequency of oscillation of the externally imposed pressure gradient. An exact solution for the axial velocity profile of a fully developed reciprocating flow is obtained from a modification of Uchida's (1950) analytical solution to give:

$$u = \frac{kD^2}{4\alpha^2 \nu}[B \cos \omega t + (1 - A) \sin \omega t] \tag{4}$$

where A and B are given, respectively, by

$$A = \frac{\mathrm{ber}\alpha\,\mathrm{bei}2\alpha\, R + \mathrm{bei}\alpha\,\mathrm{ber}2\alpha\, R}{\mathrm{ber}^2\alpha + \mathrm{bei}^2\alpha} \tag{5}$$

$$B = \frac{\mathrm{ber}\alpha\,\mathrm{ber}2\alpha\, R - \mathrm{bei}\alpha\,\mathrm{bei}2\alpha\, R}{\mathrm{ber}^2\alpha + \mathrm{bei}^2\alpha} \tag{6}$$

with $R = (r/D)$ being the dimensionless radial coordinate, and α being the Womersley number defined by

$$\alpha = \frac{D}{2}\sqrt{\frac{\omega}{\nu}} = \frac{1}{2}\sqrt{\mathrm{Re}_\omega} \tag{7}$$

where $\mathrm{Re}_\omega = (\omega D^2/\nu)$ is the kinetic Reynolds number. Integrating Equation 4 over the cross section of the pipe yields the following exact expression for the mean velocity:

$$u_m = u_{\max} \sin \phi \tag{8}$$

with $u_{\max}$ and ϕ given by

$$u_{\max} = \frac{kD^2\sigma}{32\nu} \tag{9a}$$

$$\phi = \frac{\pi}{2}(\omega t - \Lambda) \tag{9b}$$

where

$$\sigma = \frac{8}{\alpha^3}\sqrt{(\alpha - 2C_1)^2 + 4C_2^2} \tag{10a}$$

$$\Lambda = \tan^{-1}\left(\frac{\alpha - 2C_1}{2C_2}\right) \tag{10b}$$

with C_1 and C_2 in the above equations being given by

$$C_1 = \frac{\mathrm{ber}\alpha\,\mathrm{bei}'\alpha - \mathrm{bei}\alpha\,\mathrm{ber}'\alpha}{\mathrm{ber}^2\alpha + \mathrm{bei}^2\alpha} \tag{11a}$$

$$C_2 = \frac{\mathrm{ber}\alpha\,\mathrm{ber}'\alpha + \mathrm{bei}\alpha\,\mathrm{bei}'\alpha}{\mathrm{ber}^2\alpha + \mathrm{bei}^2\alpha} \tag{11b}$$

where $\mathrm{ber}'\alpha = [\mathrm{d}(\mathrm{ber}'\alpha)/\mathrm{d}\alpha]$, and $\mathrm{bei}'\alpha = [\mathrm{d}(\mathrm{bei}\ \alpha)/\mathrm{d}\alpha]$. It follows from Equations 4 and 9a that the dimensionless axial velocity for a fully developed reciprocating flow is given by

$$U = \frac{u}{u_{\max}} = f(R, \tau, \mathrm{Re}_\omega) \tag{12}$$

where $\tau = \omega t$ is the dimensionless time related to the phase angle ϕ by $\tau = 2(i-1)\pi + \phi$ with i being the number of cycle. Equation 12 shows that the dimensionless axial velocity of a fully developed flow, at a given position and time, is a function of the kinetic Reynolds number only.

We now define the instantaneous friction coefficient $c_{f,\infty}$ and the cycle-averaged friction coefficient $\bar{c}_{f,\infty}$ of a reciprocating flow as

$$c_{f,\infty}(\tau) = \frac{\tau_w(\tau)}{\frac{1}{2}\rho u_{\max}^2} = \frac{\mu\left(\frac{\partial u}{\partial r}\right)_{r=D/2}}{\frac{1}{2}\rho u_{\max}^2} \tag{13}$$

and

$$\bar{c}_{f,\infty} = \frac{1}{2\pi}\int_0^{2\pi} |c_{f,\infty}(\tau)|\, \mathrm{d}\tau \tag{14}$$

Notation

A	function defined in Equation 5
A_o	dimensionless oscillation amplitude of fluid defined in Equation 17c and 22
B	function defined in Equation 6
C_1	constant defined in Equation 11a
C_2	constant defined in Equation 11b
c_f	friction coefficient defined in Equation 13
$c_{f,\mathrm{exp}}$	measured friction coefficient defined in Equation 24
$c_{f,\mathrm{exp},j}$	measured friction coefficient at jth time interval
$\bar{c}_{f,\mathrm{exp}}$	measured cycle-averaged friction coefficient defined in Equation 25
$c_{f,\infty}$	analytical friction coefficient defined in Equation 15
$\bar{c}_{f,\infty}$	cycle-averaged friction coefficient defined in Equation 16
D	diameter of the pipe
Δp	pressure drops
F_ω	expression defined in Equations 17a and 18a
k	amplitude of the imposed pressure gradient in Equation 3
L	distance of the two taps of the pressure transducer
N_i	number of sampling intervals in one cycle
p	pressure of the fluid
r,R	dimensional and dimensionless radial coordinates
Re_ω	kinetic Reynolds number
t,τ	dimensional and dimensionless time
u,U	dimensional and dimensionless axial velocity
u_m	cross-sectional mean velocity
$u_{\max}$	maximum cross-sectional mean velocity
x	axial distance

Greek

α	Womersley number defined in Equation 7.
ϕ_1	phase difference defined in Equations 17b and 18b
Λ	phase difference defined in Equation 10b
ϕ	phase angle
ρ	density of fluid
τ_w	shearing stress at the wall
ν	kinematic viscosity of fluid
ω	oscillatory frequency

Subscripts

∞	fully developed flow
exp	measured data
f	friction
i	ith cycle
j	jth sampling interval
m	cross-sectional mean value
max	maximum value

where τ_w is the wall shearing stress. Differentiating Equation 4 and substituting in Equations 13 and 14 yield the following exact expressions for the friction coefficient of a fully developed reciprocating flow

$$c_{f,x} = \frac{32F_\omega}{A_o}\sin(\phi + \phi_1) \tag{15}$$

and

$$\bar{c}_{f,x} = \frac{64F_\omega}{\pi A_o} \tag{16}$$

with

$$F_\omega = \frac{\sqrt{C_1^2 + C_2^2}}{16\sqrt{(\alpha - 2C_1)^2 + 4C_2^2}} \tag{17a}$$

$$\phi_1 = \tan^{-1}\left(\frac{\alpha - 2C_1}{2C_2}\right) - \tan^{-1}\left(\frac{C_2}{C_1}\right) \tag{17b}$$

$$A_o = \frac{2u_{\max}}{\omega D} \tag{17c}$$

Where ϕ_1 is the phase angle difference (in degrees) between the cross-sectional mean velocity u_m given by Equation 8 and the wall shearing stress. Note that the instantaneous pressure coefficient can be either positive or negative during a cycle. The positive sign of the friction coefficient means the fluid flow moves in the positive direction, while the negative sign implies that it moves in the negative direction.

It is noted that F_ω and ϕ_1 given by Equations 17a and 17b are complicated functions of Re_ω, which are presented in Figure 1. For the convenience of computations, simplified expressions for these quantities in terms of Re_ω are needed. For this purpose, the values of F_ω and ϕ_1 computed from Equations 17a and 17b are fitted by the following algebraic expressions.

$$F_\omega = \frac{0.161}{\left(\mathrm{Re}_\omega^{0.548} - 2.039\right)} \pm 3.3\% \tag{18a}$$

$$\phi_1 = 0.647[1 - 1.015\exp(-0.019\ \mathrm{Re}_\omega)] \pm 1.9\% \tag{18b}$$

Substituting Equation 18a into Equation 16 yields

$$\bar{c}_{f,x} = \frac{3.272}{A_o\left(\mathrm{Re}_\omega^{0.548} - 2.039\right)} \tag{19}$$

which shows that the cycle-averaged friction coefficient is inversely proportional to both Re_ω and A_o.

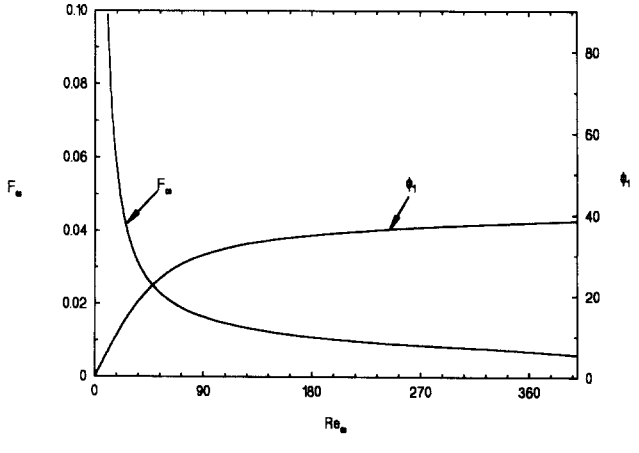

Figure 1 F_ω and ϕ_1 *versus* the kinetic Reynolds number Re_ω

Experimental details

Apparatus and instrumentation

As schematically shown in Figure 2, a closed-loop test rig, consisting of a pump, a sinusoidal motion generator, an angle position encoder, a test section (made of a long copper tube, 94.5 cm in length and 1.35 cm in diameter), four velocity straighteners, and a data acquisition system, was constructed for the present study. To have a uniform inlet velocity over the cross section and measure this velocity by a hot-wire probe, four velocity straighteners were constructed and installed at each end of the test section. The sinusoidal motion of the working fluid (air) in the test section was established by a double acting pump connected to a crank shaft and yoke sinusoidal mechanism. The pump was driven by a 1 kW DC motor with an adjustable speed. The crank shaft and yoke sinusoidal mechanism were designed so that the fluid displacement varied according to

$$x = \frac{x_{\max}}{2}(1 - \cos\phi) \tag{20}$$

where the maximum fluid displacement $x_{\max}$ can be adjusted by changing the stroke of the pump. Differentiating Equation 20 with respect to time and comparing the resulting expression with Equation 8 gives

$$u_{\max} = \frac{x_{\max}\omega}{2} \tag{21}$$

Substituting Equation 21 into Equation 17c yields

$$A_o = \frac{x_{\max}}{D} \tag{22}$$

which indicates that A_o is the dimensionless oscillation amplitude of the fluid displacement.

Pressure drops along the pipe were measured by a differential pressure transducer (Validyne, Model DP15) and a carrier demodulator (Validyne, Model CD15). To measure the pressure drops in the fully developed flow region, the pressure transducer taps were installed at locations far from the entrance of the pipe. As shown in Figure 2, the two taps of the pressure transducer separated by a distance of L ($L = 68$) were connected in the middle of the test section. To measure the cross-sectional mean velocity, a miniature hot-film probe (TSI, Model 1260A-10) was installed between the two velocity straighteners at the left side of the test section (see Figure 2). The hot-film probe was connected to a hot-wire anemometer (TSI, IFA 100) and calibrated up to a maximum velocity of 15 m/s using a calibrator (Model 1125, TSI). The calibrator accuracy is $\pm 2\%$ for velocities between 3 to 300 m/s, $\pm 5\%$ for velocities in the range of 0.15 to 2 m/s, and $\pm 10\%$ for velocities below 0.15 m/s. Analog-to-digital conversions were carried out by a Metrabyte DAS-20 A/D board, giving 100,000 samples per second with 12-bit precision. A 4-channel simultaneous sample and hold front end for the A/D board (Metrabyte, SSH-4) was employed, which was capable of securing the 4-channel signals to be sampled simultaneously. The phase angle ϕ was monitored by an optical shaft encoder (Lucas Ledex, Model LD23) with two degree resolution, which could also provide a top dead center (TDC) signal for data acquisition purposes. Thus, both the velocities and pressure drop signals were sampled with two-degree resolution over 180 intervals in one period starting at TDC.

Data reduction

As mentioned earlier, pressure drops were measured in the fully developed flow region. Therefore, the reduction of experimental data is based on a hydrodynamically fully developed flow whose momentum equation is given by Equation 2. If Equation 2 is first

multiplied by $2\pi r dr$ and integrated over the cross section of the tube and then integrated with respect to x from $x = 0$ to $x = L$, it becomes

$$\frac{\Delta p}{L} = \rho \frac{du_m}{dt} + \frac{4\tau_w}{D} \tag{23}$$

where we have assumed $(\partial p/\partial x)$ is a constant. Substituting Equation 23 into Equation 13 and solving for $c_{f,\exp}$ yields

$$c_{f,\exp} = \frac{1}{2\rho u_{\max}^2}\left(\Delta p \frac{D}{L} - \rho D \frac{du_m}{dt}\right) \tag{24}$$

where Δp and u_m can be measured by the differential pressure transducer and the hot-wire anemometer, respectively. In the present study, the data were analyzed using the ensemble-averaged pressure drop and cross-sectional mean velocity. The number of the samples to be ensembly averaged was 100 cycles. The measured cycle-averaged friction coefficient $\bar{c}_{f,\exp}$ is defined as

$$\bar{c}_{f,\exp} = \frac{1}{N_1}\sum_{j=1}^{N_1} |c_{f,\exp,j}| \tag{25}$$

where N_j is the total number sampling intervals in a cycle, and $c_{f,\exp,j}$ is the data evaluated based on Equation 24 at the jth interval.

Uncertainty analysis

An uncertainty analysis based on the method described by Moffat (1988) was performed. Uncertainty in the kinetic Reynolds number Re_ω was dominated by the measurement of oscillation frequencies and was estimated at $\pm 2.3\%$. Uncertainty in the dimensionless oscillation amplitude of the fluid A_o was computed to be less than $\pm 0.5\%$, which was primarily influenced by errors in measuring the stroke and the diameter of the air pump. The main source of errors in the reported results of the friction coefficient is statistical uncertainty in the ensemble-averaged quantities of velocities and pressure drops due to the finite number of measurements. The statistical uncertainty in the ensemble-averaged velocity is estimated to be $\pm 4.5\%$, assuming uncorrelated, normally distributed measurements with a 95% confidence level. Similarly, the statistical uncertainty in the ensemble-averaged pressure drops varies from ± 6 to $\pm 9\%$. The largest uncertainties in the measurements of the cycle-averaged friction coefficient $\bar{c}_{f,\exp}$ were computed to be about $\pm 10.5\%$.

Results and discussion

In this section, we present analytical and experimental results of the instantaneous and cycle-averaged friction coefficients for a laminar reciprocating flow of air in a long circular pipe. Experiments on pressure drops downstream of a long pipe were carried out for $A_o \leq 26.42$ and with the value of Re_ω ranging from 23.1 to 395 where the velocity profiles appeared to be laminar.

Figure 3 is a comparison of the assumed sinusoidal cross-sectional mean velocity u_m given by Equation 8 and the measured ensemble-averaged velocity at the inlet of the tube at $\mathrm{Re}_\omega = 208.2$

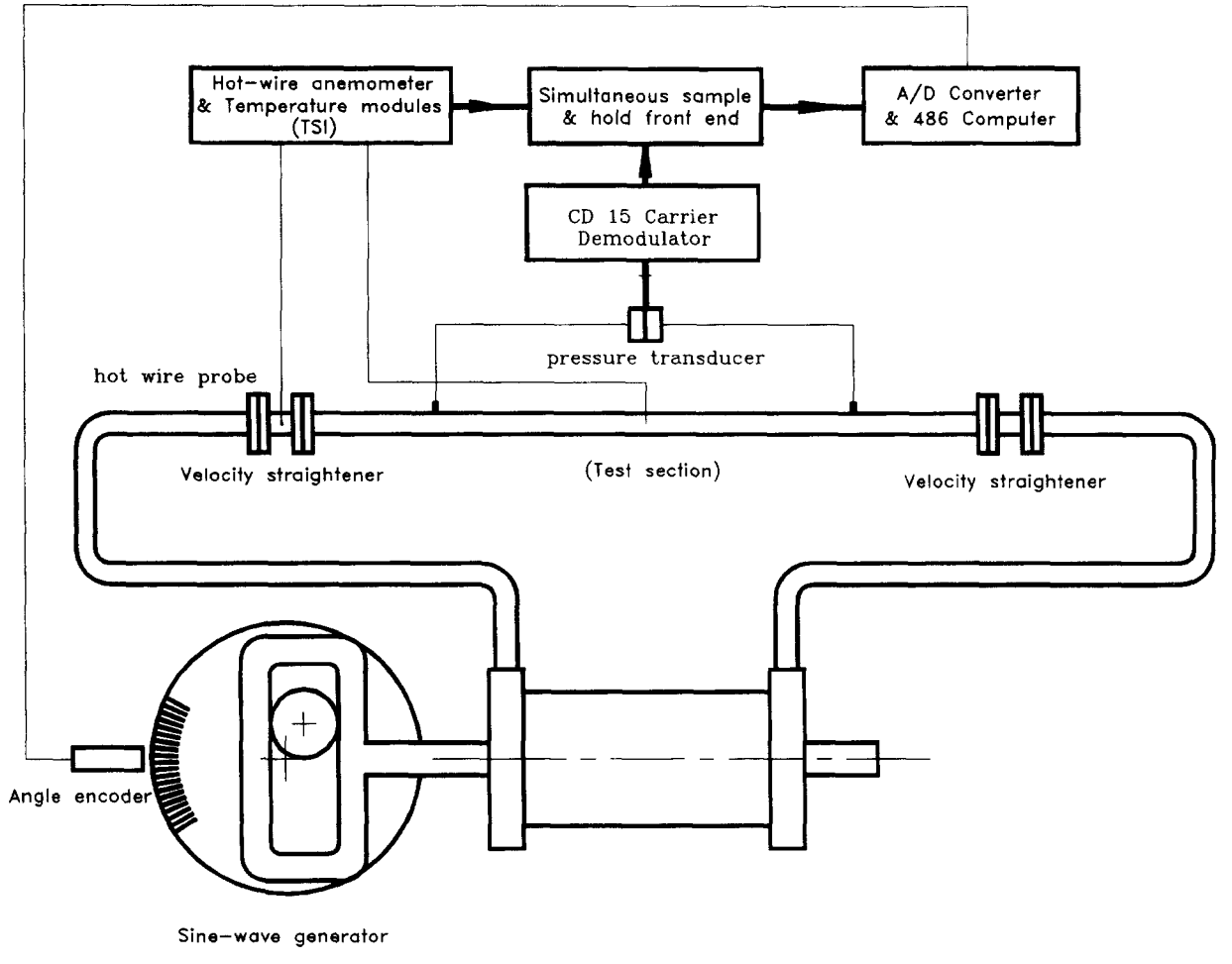

Figure 2 Schematic diagram of the apparatus

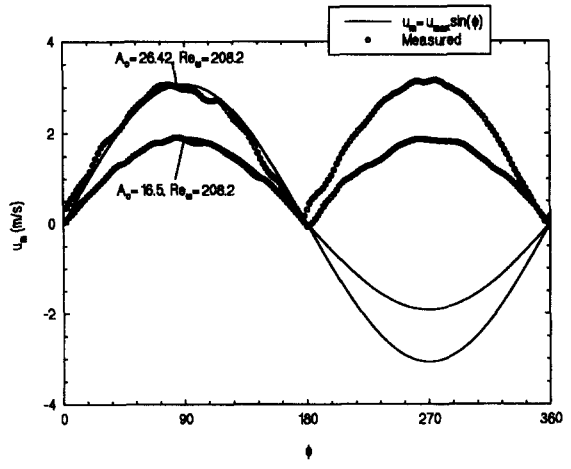

Figure 3 Comparison of the ensemble-averaged traces of the cross-sectional mean velocity at the inlet and the assumed sinusoidal inlet mean velocity variation

for $A_o = 16.5$ and 22.51. It is shown that for the smaller value of $A_o (A_o = 16.5)$ the measured velocity is in good agreement with the assumed sinusoidal cross-sectional mean velocity of the analytical solution. However, for higher values of $A_o (A_o = 22.51$, for example), the measured velocities deviated slightly from the sinusoidal curve at certain instances of time. Uncertainty in the ensemble-averaged velocity is $\pm 2.5\%$. It is worth mentioning that, because the hot-wire probe could not detect the flow direction, the velocity shown in the figure is the absolute value.

Typical variations of the measured instantaneous pressure drops during a complete cycle at $A_o = 26.42$ for $\mathrm{Re}_\omega = 144.1$ and $\mathrm{Re}_\omega = 324.3$ are illustrated in Figure 4. It is seen that the pressure drops increase with the increase of the kinetic Reynolds number at a fixed value of dimensionless oscillation amplitude of the fluid. Two main reasons may be attributed to the increase of the pressure drops under these conditions. First, the increase of the kinetic Reynolds number leads to more significant "annular effect" and thus the radial velocity gradients adjacent to the pipe wall become steeper; consequently, the friction force increases with the increase of the kinetic Reynolds number. Second, the inertia component in the momentum balance increases with the increase of the kinetic Reynolds number.

Figure 5a shows typical variations of the instantaneous friction coefficient c_f during a complete cycle at $A_o = 16.5$ for $\mathrm{Re}_\omega = 64$ and $\mathrm{Re}_\omega = 208.2$, and Figure 5b shows those at $\mathrm{Re}_\omega =$

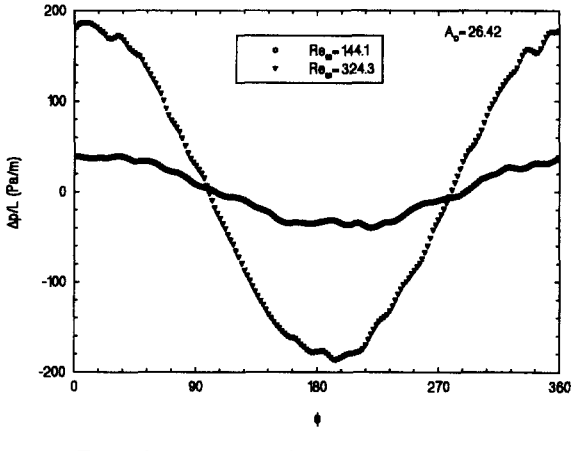

Figure 4 Typical variations of the ensemble-averaged pressure drops for $\mathrm{Re}_\omega = 144.1$ and 324.3 at $A_o = 10$

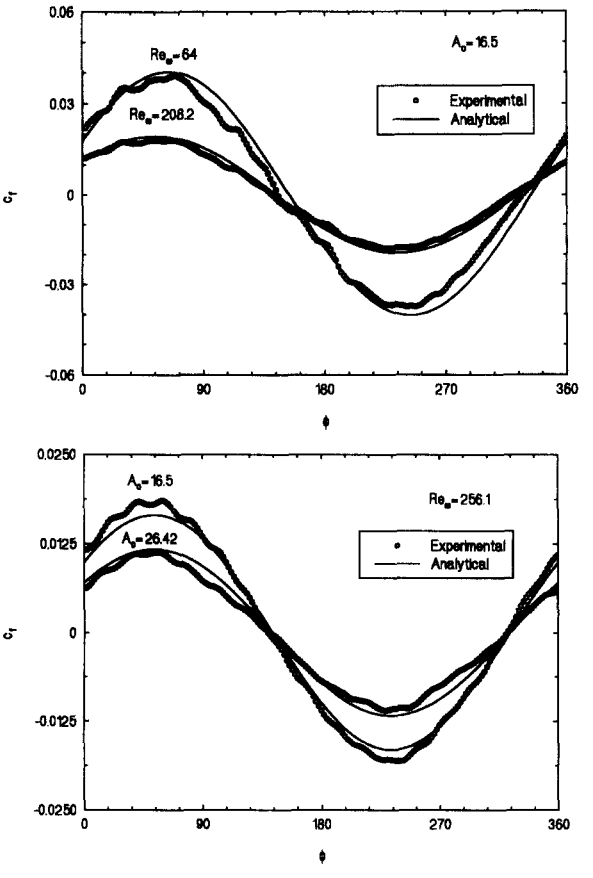

Figure 5 (a) Comparison of the instantaneous friction coefficient of the fully developed flow between analytical and experimental results for $\mathrm{Re}_\omega = 64$ and 208.2 at $A_o = 10$; (b) Comparison of the instantaneous friction coefficient of the fully developed flow between analytical and experimental results for $A_o = 16.5$ and 26.42 at $\mathrm{Re}_\omega = 256.1$

256.1 for $A_o = 16.5$ and $A_o = 26.42$. The circle symbols represent the measured data $c_{f,\mathrm{exp}}$, and the solid lines represent the analytical solutions $c_{f,\infty}$, given by Equation 13, at the corresponding conditions. Generally, the temporal friction coefficient varies sinusoidally, and its amplitude decreases with either the increase of the kinetic Reynolds number at a fixed value of the dimensionless oscillation amplitude of the fluid (shown in Figure 5a) or the

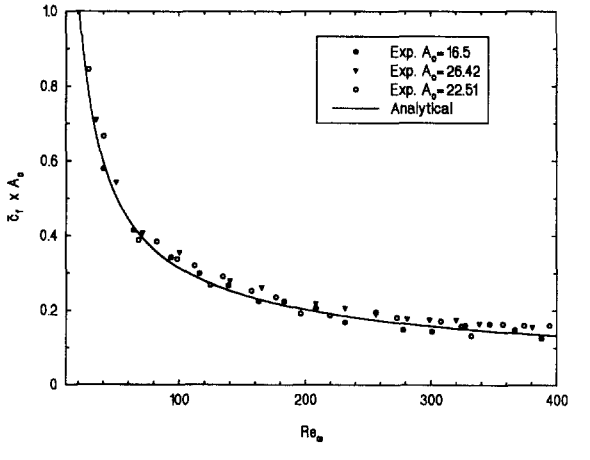

Figure 6 Comparison of the cycle-averaged friction coefficient between analytical solution and experimental data

increase of the dimensionless oscillation amplitude of the fluid at a fixed value of the kinetic Reynolds number (shown in Figure 5b). Comparing the analytical solution with the measured data, we can see that the analytical solution is in a fairly good agreement with the experimental data.

A comparison of the cycle-averaged friction coefficient of the measured data $\bar{c}_{f,\exp}$ and the analytical solution $\bar{c}_{f,\infty}$ given by Equation 19 for $A_o = 16.5$, 22.51, and 26.42 is presented in Figure 6. The symbols represent the measured data, and the solid line represents the analytical solution. It is shown that the analytical solution is in good agreement with the experiment, with the maximum deviation from the analytical solution being $\pm 14.8\%$. The scatter of data may be attributed to the fact that fluctuations occurred in the measurements of pressure drops and cross-sectional mean velocities, as shown in Figures 3 and 4.

Concluding remarks

In this paper, it is shown that a sinusoidally reciprocating flow in a long pipe is governed by two similarity parameters: the dimensionless oscillation amplitude of fluid, and the kinetic Reynolds number. Analytical expressions for the instantaneous and cycle-averaged friction coefficients of a fully developed laminar reciprocating pipe flow have been obtained in terms of these two parameters. These simple expressions for the friction coefficients of a laminar reciprocating flow are shown to be in good agreement with measurements.

References

Akhavan, R., Kamm, R. D. and Shapiro, A. H. 1991. An investigation of the transition to turbulence in bounded oscillatory stokes flows, Part 1: Experiments. *J. Fluid Mech.* **225**, 423–444

Moffat, R. J. 1988. Describing the uncertainties in experimental results. *Exp. Thermal Fluid Sci.* 3–17

Richardson, E. G. and Tyler, E. 1929. The transverse velocity gradient near the mouths of pipes in which an alternating or continuous flow of air is established. *Proc. Phys. Soc. London*, **42**, 1–15

Roach, P. D. and Bell, K. J. 1988. Analysis of pressure drop and heat transfer data from the reversing flow test facility. Report # ANL/MCT-88-2, Argonne National Laboratory, Argonne, IL

Sexl, T. 1930. Uber den von entdeckten Annulareeffekt. *Zeitschrift fuer Physik*, **61**, 349–362

Taylor, D. R. and Aghili, H. 1984. An investigation of oscillating flow in tubes. *Proc. 19th Intersociety Energy Conversion Engineering Conference* (IECEC Paper 84916), pp. 2033–2036, American Nuclear Society

Uchida, S. 1950. The pulsating viscous flow superposed on the steady laminar motion of an incompressible fluid in a circular pipe. *ZAMP*, 7, 403–422

Womersley, J. R. 1955. Method for the calculation of velocity, rate of the flow, and viscous drag in arteries when the pressure gradient is known. *J. Physiol.* **127**, 553–563

Wu, P., Lin, B., Zhu, S., He, Y., Ren, C. and Wang, F. 1990. Investigation on oscillating flow resistance and heat transfer in the gap used for cryocoolers. *Proc. 13th Intersociety Energy Conversion Engineering Conference*